International Journal of Applied Earth Observation and Geoinformation 31 (2014) 110–121

Contents lists available at ScienceDirect

International Journal of Applied Earth Observation and Geoinformation

journal homepage: www.elsevier.com/locate/jag

Object based change detection of Central Asian Tugai vegetation with very high spatial resolution satellite imagery

Philipp Gärtner[a,*], Michael Förster[a], Alishir Kurban[b], Birgit Kleinschmit[a]

[a] Geoinformation in Environmental Planning Lab, Technische Universität Berlin, Berlin 10623, Germany
[b] Xinjiang Institute of Ecology and Geography, Chinese Academy of Science, Urumqi 830046, China

ARTICLE INFO

Article history:
Received 2 October 2013
Accepted 10 March 2014
Available online 12 April 2014

Keywords:
Tree detection
Tree crown delineation
QuickBird
WorldView2
Riparian forest
Populus euphratica

ABSTRACT

Ecological restoration of degraded riparian Tugai forests in north-western China is a key driver to combat desertification in this region. Recent restoration efforts attempt to recover the forest along with its most dominant tree species, *Populus euphratica*. The present research observed the response of natural vegetation using an object based change detection method on QuickBird (2005) and WorldView2 (2011) data. We applied the region growing approach to derived Normalized Difference Vegetation Index (NDVI) values in order to identify single *P. euphratica* trees, delineate tree crown areas and quantify crown diameter changes. Results were compared to 59 reference trees. The findings confirmed a positive tree crown growth and suggest a crown diameter increase of 1.14 m, on average. On a single tree basis, tree crown diameters of larger crowns were generally underestimated. Small crowns were slightly underestimated in QuickBird and overestimated in Worldview2 images. The results of the automated tree crown delineation show a moderate relation to field reference data with R^2_{2005}: 0.36 and R^2_{2011}: 0.48. The object based image analysis (OBIA) method proved to be applicable in sparse riparian Tugai forests and showed great suitability to evaluate ecological restoration efforts in an endangered ecosystem.

1. Introduction

Ecological restoration of degraded riparian Tugai forests in north-western China is a key driver to combat desertification in this region. Past and current restoration efforts attempt to recover the forest along the Tarim river with its most dominant tree species, Euphrates Poplar *(Populus euphratica)*, which provides desirable services to the local ecosystem such as sand fixation, wind break, and riverbank protection (Weisgerber, 1994). The response of the natural vegetation to applied restoration decisions are of particular interest to restoration managers, who seek for accurate long-term monitoring which requires the detection of change and quantification of its rate (Coppin et al., 2004).

Current field-survey methods deliver accurate data for the detection and quantification of forest change but may not be suitable for long-term and large scale monitoring due to low sample coverage and infrequent survey opportunities (Pouliot et al., 2002). Furthermore, in large arid or semi-arid areas, where vegetation cover is usually sparse and scattered, field surveys become time-consuming and cost intensive. In this context, remote sensing offers several desirable characteristics from a forest restoration monitoring perspective including large footprint sizes, and regular data collection cycles (Chubey et al., 2006). Nevertheless, the potential to detect changes in forest ecosystems are intrinsically limited by the satellite images spatial resolution (Coppin et al., 2004). Generally, medium spatial resolution (~30 m) sensors such as Landsat, SPOT, or ASTER have the potential to monitor changes in large forest stands (>10 ha). Typical approaches detect forest cover change due to clear cuttings (Desclée et al., 2006) or selective harvesting (Kennedy et al., 2007; Sader et al., 2003). The results are reliable and have been, for instance, operationally utilized by the Swedish Forest Agency to verify cutting permits (Olsson et al., 2005).

With the launch of QuickBird2 (QB) (2001), GeoEye-1 (2008), and WorldView2 (WV2) (2009), data from three satellites with very high spatial resolution (VHSR) sensors are available. This changed the opportunities for the analysis of forest ecosystems using remote sensing and shifted the scale of interest from forest stands down to the individual tree level (Falkowski et al., 2009). The spatial resolution in a sub-meter dimension (<0.8 m) allowed reliable computation of several forest inventory parameters such as canopy closure (Leckie et al., 2005), stem density (Hirata, 2008), and crown size (Ozdemir, 2008). Combining VHSR data with the height

* Corresponding author. Tel.: +49 30 314 27851.
E-mail addresses: philipp.gaertner@tu-berlin.de, gaertner.p@gmail.com (P. Gärtner), michael.foerster@tu-berlin.de (M. Förster), alishir@ms.xjb.ac.cn (A. Kurban), birgit.kleinschmit@tu-berlin.de (B. Kleinschmit).

http://dx.doi.org/10.1016/j.jag.2014.03.004
0303-2434/

information from light detection and ranging (LiDAR) data allowed accurate recognition of tree crowns and the determination of tree height (Leckie et al., 2003b), tree volume (Mora et al., 2013), and, by means of allometric equations, improved estimations of the above ground forest biomass and carbon stocks (Bright et al., 2012). However, its operational implementation in forest ecosystem analysis is still limited due to the high cost for large area surveys.

In VHSR imagery, the target entity (individual tree) is normally composed of several pixels with a high degree of spatial detail. In order to allow meaningful image analysis, groups of homogeneous pixels need to be aggregated into one object, the individual tree object. The aggregation process suggested a change from traditional pixel based image analysis towards an object based image analysis (OBIA) (Blaschke, 2010). With the OBIA approach, each image tree object can be described by its spectral characteristics as well as spatial features such as shape, position, size, and the relationship to neighbouring objects (Blaschke et al., 2011) and hence allowed the development of semi-automated algorithms for tree cover information extracted for each tree entity. The core of the developed information extraction algorithms relies on sub processes such as (a) tree crown detection and (b) tree crown delineation, whereas for some methods, tree crown detection is a required step prior to crown delineation (Ke and Quackenbush, 2011b).

A range of methods for tree crown detection exist in the literature including local maximum (LM) filtering (Gebreslasie et al., 2011; Wulder et al., 2000, 2004), scale analysis (Pouliot et al., 2005), template matching (Niccolai et al., 2010) and directional local filtering (van Coillie et al., 2012). An emerging approach is the LM filtering which applies a moving window and takes the pixel with the maximum value to represent the treetop (Pouliot et al., 2002). A key matter remains the size of the moving-window which is dependent on the relationship between the tree-crown dimension and spatial resolution of the image (Gougeon and Moore, 1988). A previous study from Gebreslasie et al. (2011) used a panchromatic IKONOS image for the detection of tree location in a plantation forest with mainly flooded gum (*Eucalyptus grandis*) in KwaZulu-Natal, South Africa. The approach included Gaussian smoothing, and vegetation masking prior two LM filtering approaches with: (a) a variable window size selection based on semivariogram techniques and (b) a standard fixed window size. In young dense plantation forest the variable window size approach achieved 75% detection accuracy. The accuracy increased (up to 90%) with increasing tree age and decreasing tree density. However, the fixed window size LM filtering approach achieved 67% detection accuracy in young forest stands and up to 88% in the older stands.

Wulder et al. (2004) compared LM filtering for the identification of individual trees on a 1 m airborne MEIS II and a 1 m IKONOS image in a plantation forest and a mature stand of Douglas fir (*Pseudotsuga menziesii*) and western red cedar (*Thuja plicata*) in Canada. The LM filtering with variable window size performed poorly on the IKONOS image, resulting in low overall accuracy (61%) and large errors of commission (48%). However, the results from the LM filtering with a 3×3 fixed window size on the IKONOS image indicated that individual trees were identified with greater accuracy (85%). A LM filter with a fixed window size is used in the present study.

Tree crown delineation algorithms are based on the underlying assumption that crown tops have higher spectral reflectance than the lower parts of the crown, particularly at the boundaries between crowns (Katoh and Gougeon, 2012). Today, a variety of methods for tree crown delineation exist and can be generally categorized into, valley following (Gougeon and Leckie, 2006; Leckie et al., 2003a), region growing (Bunting and Lucas, 2006; Culvenor, 2002; Pouliot et al., 2002; Tiede et al., 2008) and watershed segmentation (Wang et al., 2004). The region growing method is a threshold-based clustering approach which requires the maxima-derived treetops from the LM filter approach as starting point and a specified threshold value as boundary constraint (Culvenor, 2002). Examples of region growing applications can be found in open mixed species forest with crowns of differing crown shape and size (Bunting and Lucas, 2006) or even aged Mountain Ash forest (*Eucalyptus regnans*) (Culvenor, 2002), both in Australia.

Change detection of tree crown objects with VHSR satellite imagery have been developed recently (Ardila et al., 2012b,a; van der Sande, 2010). Ardila et al. (2012a) introduced a multi-temporal detection strategy based on active contours to monitor urban tree crowns in a series of very high resolution (VHR) aerial images in Enschede and Delft, The Netherlands. The identification of abrupt and gradual tree crown changes was computed on a one-to-one object comparison which performed superior to an alternative region growing segmentation approach. Another promising methodology was introduced by Ardila et al. (2012b), where crown changes as well as change uncertainty of trees in an urban environment Enschede and Delft are quantified. Their method iteratively fits a Gaussian function to crown membership in QB and aerial images of two dates and afterwards identified tree crown elliptical objects. For the retrieved tree crown objects crisp changes are identified. Additionally, change uncertainties are computed based on fuzzy membership functions which take spatial characteristics and mixed-pixel effects of tree crown pixel locations into account. Both previous studies were applied in urban environments and used visual interpretation and digitization of the input images as reference data for quantitative performance evaluation.

While there have been studies assessing multi-temporal change detection of urban trees, to our knowledge no studies investigated long-term changes of degraded open Tugai forest based on single tree crowns with VHSR imagery and neither were they validated with field-based crown diameter measurements. Therefore, the objective of this study was to apply the OBIA approach to quantify tree crown changes based on object to object comparison using VHSR imagery (QB and WV2). The study area was a Central Asian Tugai forest in the lower reaches of the Tarim River in northwest China, which experienced recent revitalization due to ecosystem restoration efforts. Accuracies for tree crown diameter measures are produced and compared to reference data of visual tree delineation and field-based tree crown measurements. Finally, we indicate the suitability of the proposed method with regards to ecosystem restoration evaluation purposes. The following research questions were addressed in this study:

1. How did *P. euphratica* tree crowns develop during 2005 and 2011 in the lower reaches of the Tarim River?
2. How accurate are OBIA tree crown delineation results in comparison to (a) visually interpreted and digitized and (b) terrestrial tree crown measurements?

2. Method

2.1. Study area

The study area (Fig. 1) is located at the Arghan forest station in the Xinjiang Uyghur Autonomous Region in north-west China where the old Tarim River and the Qiwinköl Tarim branch merge (N 40°8.72′ E 88°21.26′). The regional climate shows extreme arid characteristics with precipitation below 50 mm and potential evaporation above 2000 mm. per annum (Chen et al., 2006a). Average monthly temperatures vary from just under −12 °C in January, to over 27 °C in July, while the annual average is at 11.7 °C. The area is dominated by open sandy areas with dense clusters of *P. euphratica* along the riverbanks and to sparse isolated trees towards the desert. A forest inventory in 2004/2005 revealed that about 4500 *P. euphratica* trees exist within the study area (Lam et al., 2011).

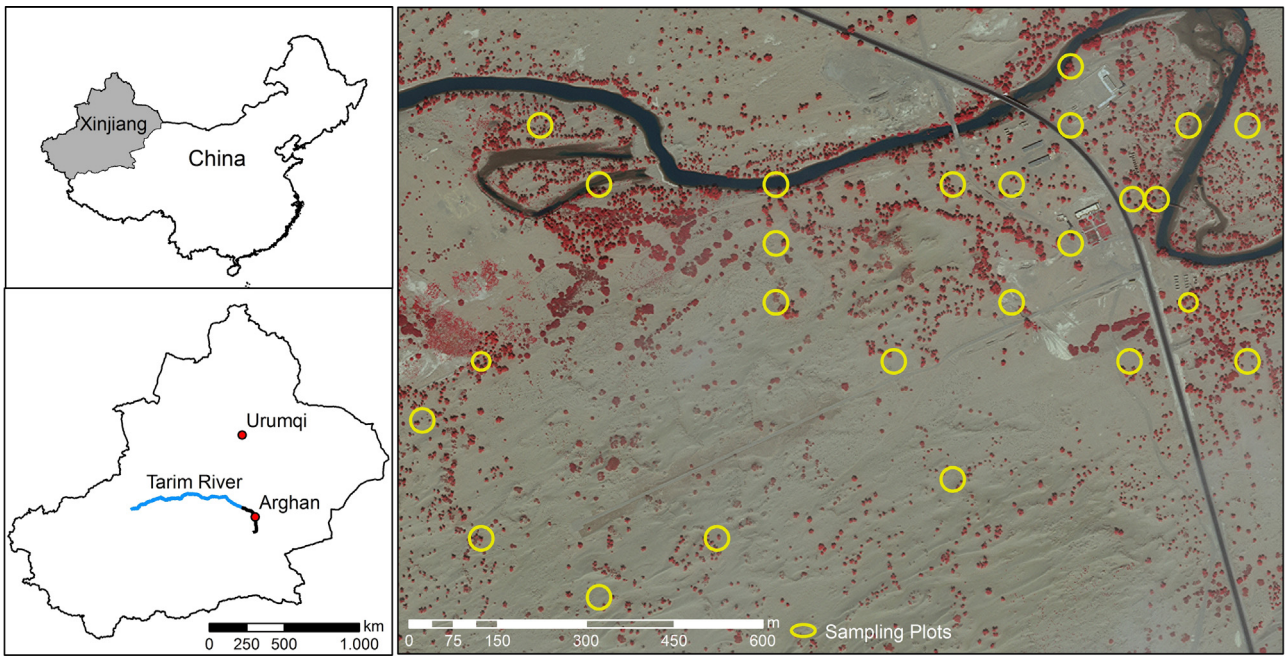

Fig. 1. Location of the Xinjiang Uyghur autonomous region in China (upper left); study area at Arghan, along the lower reaches of Tarim River Basin (black line) in Xinjiang Uyghur autonomous region (lower left); Location of 25 randomly selected field plots established by Lam et al. (2011) (background image: WV2, date: 29/07/2011, false colour composite) (right).

Common shrub species in the area include *Tamarix ramosissima*, *Tamarix hispida*, *Tamarix leptostachys*, *Elaeagnus angustifolia*, and *Karelina caspica*. These are all drought-enduring and salt-tolerant species (Zhou et al., 2010), however as phreatophytes their roots need continuous contact to groundwater for their growth and survival (Thevs et al., 2012). Although there are some old stumps, no silvicultural management operations have been carried out and the forest can be considered to be in a semi-natural stage. The area represents the characteristic floristic composition and health situation of Tugai floodplain vegetation at the lower reaches of the Tarim river.

2.2. Ground reference data

The open Tugai vegetation in the research area was mapped in a stratified random sample covering the full range of vegetation diversity and density. For a consistent and comparable long time monitoring, 25 permanent sampling plots were established in 2005 (Lam et al., 2011) (Fig. 1). The default plot radius was 20 m. In areas with fewer large trees, the plot size was decreased to 15 m. Within the sampling plots, 62 reference trees were randomly selected and their height, diameter at breast height (DBH), and crown diameter were measured. The measurements were conducted in the summer of 2005 and 2011 during the vegetation's maximum development phase. Tree crown diameters were derived by projecting the edges of the crown to the ground and measuring the length of the longest canopy axis (major axis) and the crown axis perpendicular to this axis (minor axis). The average of both values provides the mean crown diameter, a single summary value to evaluate image crown delineations.

2.3. Image acquisition and preprocessing

Two very high resolution satellite imageries from 2005 and 2011 were used in this work. On 20th of July 2005, the QB satellite acquired an image of the study area in four spectral bands covering blue, green, red, and near-infrared (NIR). The WV2 satellite recorded the same area on 29th of July 2011. Beside the four standard bands (blue, green, red, NIR), the WV2 imagery also contains 4 additional bands (coastal 0.400–0.450 μm, yellow 0.585–0.625 μm, red-edge 0.705–0.745 μm, and additional near-infrared 0.860–1.040 μm). The data provider resampled the panchromatic ground resolution to 0.6 m (QB) and 0.5 m (WV2) and multispectral resolution to 2.4 m (QB) and 2.0 m (WV2) and radiometrically corrected the image pixels before delivery. Because both sensors are in sun synchronous orbit their nodal crossing time is similar (see Table 1). The difference of nine days between the acquisition dates result in a 1.41 min shift in acquisition time and hence in a slightly different sun elevation and azimuth. However, the major dissimilarity between the images is the off nadir view angle. The view angle of the QB scene is 12.5° while the WV2 off nadir angle is about 5.2° larger.

We corrected the images geometrically and calculated top of atmosphere reflectance values using sensor and band specific calibration factors (Krause, 2005; Updike and Comp, 2010). The Hyperspherical Colour Sharpening (HCS) (Padwick et al., 2010)

Table 1
Main acquisition parameters for QB and WV2 images.

	Date of acquisition	Acquisition time (GMT)	Spatial resolution (panchromatic/ multispectral) (m)	Sun elevation angle (°)	Sun azimuth angle (°)	Off-Nadir view angle (°)	Sensor azimuth angle (°)
QB	07/20/2005	05:12:53	0.6/2.4	66.9	142.0	12.5	207.7
WV2	07/29/2011	05:14:34	0.5/2.0	65.4	144.9	17.7	55.1

algorithm was applied to fuse the multispectral and panchromatic bands into one multispectral dataset with a final spatial resolution of 0.6 m (QB) and 0.5 m (WV2). For the analysis were normalized difference, ratio-based and soil-line-related vegetation indices calculated and employed. Apart from the original normalized difference vegetation index (NDVI) (Tucker, 1979), its red edge adaptation (NDVI-RE) (Gitelson and Merzlyak, 1994) and its modified form (Mod-NDVI-RE) (Sims and Gamon, 2002) was the Green NDVI (Gitelson et al., 1996) and the normalized difference water index (NDWI) (McFeeters, 1996) created. As ratio-based vegetation index served the Simple Ratio Index (SRI) (Jordan, 1969). The used soil-line vegetation indices were the soil-adjusted vegetation index (SAVI) (Huete, 1988) its modified form (MSAVI) (Qi et al., 1994) and its optimized form (OSAVI) (Rondeaux et al., 1996).

The NDVI layer was used to create a vegetation mask using a multi-threshold segmentation which splits and classifies image objects based on a automatic NDVI threshold selection. The algorithm uses a combination of histogram-based methods and the homogeneity measurement of multi-resolution segmentation to calculate a threshold dividing the selected set of pixels into two subsets, so that heterogeneity is increased to a maximum (eCognition, 2012b).

2.4. OBIA approach for change detection

The change detection approach we present here was applied to both acquired images and combines six sequential steps to: (2.4.1) classify tree, shrub and grassland areas; (2.4.2) detect individual tree seed points with local maxima values, (2.4.3) delineate seeds into tree crown object, (2.4.4) post-process tree crown objects, (2.4.5) quantitatively assess the tree detection and crown delineation, and finally (2.4.6) calculate detected changes between 2005 and 2011.

2.4.1. Vegetation classification

Tree crown identification is largely affected by the low spectral separability of tree crown pixels with respect to other vegetated surfaces such as shrub and grass cover, which impede the correct identification and delineation of tree crowns (Ardila et al., 2012a). Hence, our first step was to identify shrub and grassland cover and exclude them prior to tree detection (Fig. 2). In total 407 training areas were manually selected based on field information and visual image interpretation (tree cover: 170, shrub cover: 175 and grassland cover: 62). The Classification and Regression Tree (CART) classifier was used to build a decision tree model with mean values of the original spectral bands of the QB and WV2 sensor and mean values of vegetation indices, listed in Section 2.3. The classifier creates a binary tree model with maximal depth using the impurity Gini index (Breiman et al., 1984) and prunes it back to obtain the optimal tree by determining the lowest misclassification errors (Laliberte et al., 2007). We allowed a maximum tree depth of 6 nodes with a minimum number of 5 samples per node, and a 6-fold cross validation. Based upon the produced decision tree model, threshold values for separating the three classes could be afterwards implemented as a rule set in the eCognition (Trimble Geospatial, version 8.8.) software.

2.4.2. Tree crown detection

Under normal conditions is the crown peak of deciduous trees more likely to be directly illuminated, and has therefore higher spectral reflectance than the crown edge (Culvenor, 2002). To identify probable *P. euphratica* crown peaks we applied a pixel based minimum/maximum filter on the NDVI layer. The filter effectively accentuates crown edges with high values while values drop in areas where the NDVI increases and plunge to zero at NDVI maximum. Next, without using hard coded NDVI thresholds, we assigned filter pixels with the value 0 (highest NDVI value) as crown peak. In comparison to conifers, the *P. euphratica* crown can be morphologically characterized as relatively flat. Therefore, we considered pixels in the immediate vicinity of the declared crown peaks and with a filter value below or equal to 0.03 to belong to the crown peak (Fig. 3 – top row). We restricted the search domain to the previously created tree cover area and fixed the search range to 7×7 pixels filter window.

2.4.3. Tree crown delineation

To delineate crown peaks into individual tree cover objects we applied a threshold based region growing approach implemented in the Conditional Quad Tree segmentation (eCognition, 2010). The procedure iteratively segments tree cover objects into quadtree grids consisting of squares (eCognition, 2012a) where the user defined conditions of (a) minimum object size (1) and (b) adjacent existence of crown peak objects are met (Fig. 3 – middle row). Next, crown peak objects grew into or merged with neighbouring tree cover objects if the mean NDVI difference was below a predefined threshold ($\leq$0.01). With each iteration grew the crown peak larger until the boundary of the tree cover (step A) was reached or a neighbouring crown blocked its growth (Fig. 3 – bottom row). Crown peaks adjacent to one another were merged in the first two steps of region growing.

2.4.4. Post processing

Tree crown borders were smoothed using a morphology operation which applied a binary mask. Image objects completely containing the mask were added to the tree crown and smaller holes inside the tree crowns were filled.

The appearance of tree crowns in VHSR satellite imagery are affected by the sun illumination angle and the sensor off nadir view angle (Song et al., 2010). As the off nadir viewing increases the size of the projected tree crown in the image, we used a view angle correction factor F in order to have comparable crown delineation results of the QB and WV2 sensors. The angle correction was applied for the statistics and did not alter the crown objects. Factor F was obtained by dividing 1 by the cosine from the sensor off nadir view angle called theta [$F = 1/\cos(\text{theta})$].

2.4.5. Accuracy assessment

For validation of tree detection and crown delineation we used: (a) manually digitized crowns as reference crowns and (b) field measured crown diameters as ground truth. The tree detection error was analyzed at the individual tree level. We computed the ratio between reference crowns to crown seeds from the local maxima approach (adapted from Leckie et al. (2004) modified by Ke and Quackenbush (2011a)). In our study, error of omission was counted when no seed was identified within the boundary of an existing reference crown (0 seed: 1 reference tree) and error of commission was registered when a seed was within an image object other than a reference tree (1 seed: 0 reference tree). We considered a tree as correctly identified when a single seed was completely within one reference tree boundary (1 seed: 1 reference tree). Two or more seeds in one reference tree illustrated a commission error, this case was registered as 2:1 (or $\geq$3: 1 for three or more seeds) correspondence. In the case where a group of trees (e.g. three trees) was erroneously covered by a single seed, the corresponding ratio would have been 1:3 (1 seed: 3 reference trees).

To compare field measured crown diameter vs. automated crown diameter we performed an analysis of linear regression outliers to determine those field measured crown diameter values that were likely to be a measurement error. These outliers were excluded from the analysis. In order to quantify crown measurement errors, we compared the mean crown diameter from the

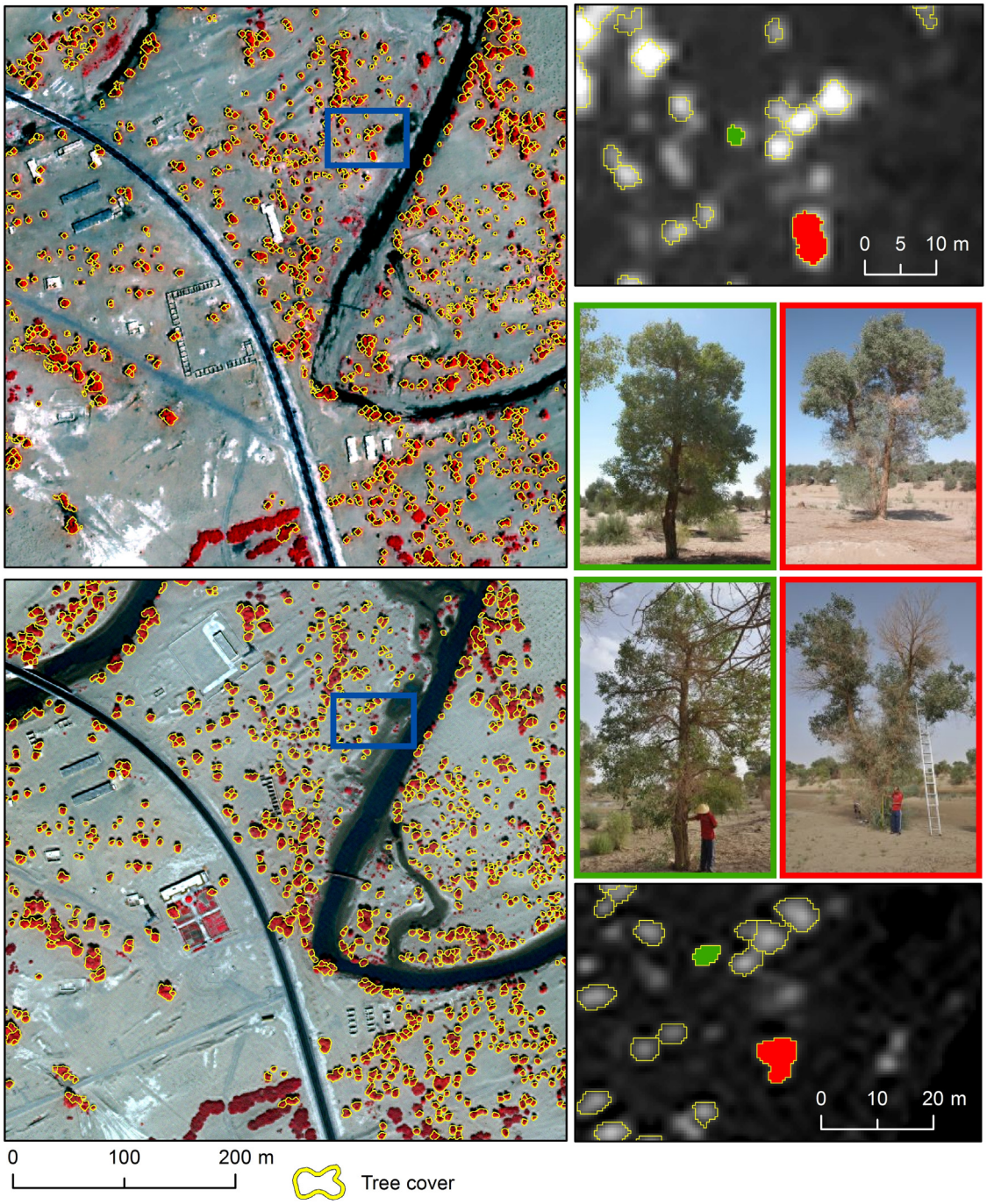

Fig. 2. *P. euphratica* tree cover of the study area in false colour composite images (QB – 2005 – upper left, WV2 – 2011 – lower left) with image inlets of their corresponding NDVI (dark – low values, bright – high values). Tree photographs (upper row – 2005, lower row – 2011) correspond to green and red vectors.

automatically extracted and manually digitized tree crowns with the averaged field measured crown diameter. The root mean square error (RMSE) and a coefficient of determination R^2 were used to quantify the deviation of tree crown diameters between remote sensing derived crowns (automatically extracted and manually digitized) and field measured crowns.

2.4.6. Change calculation

We selected in each image delineated reference tree crowns and measured the major axis (passing through the tree peak) and the perpendicular minor axis of the tree crowns. The arithmetic mean of both values marked the image based crown diameter. We compared the image derived crown diameter between the 2005 and 2011 and calculated the detected changes.

3. Result

From the 4500 inventoried *P. euphratica* trees were about 3610 (80.2%) in the QB and around 3455 (76.7%) in the WV2 imagery successfully recognized. Between 2005 and 2011 disappeared 180 trees and 25 new trees were identified. However, the average tree cover increased from 26.77 m^2 to 31.22 m^2 between 2005 and 2011. The following sections describe the results of the undertaken change analysis focusing solely on the reference trees.

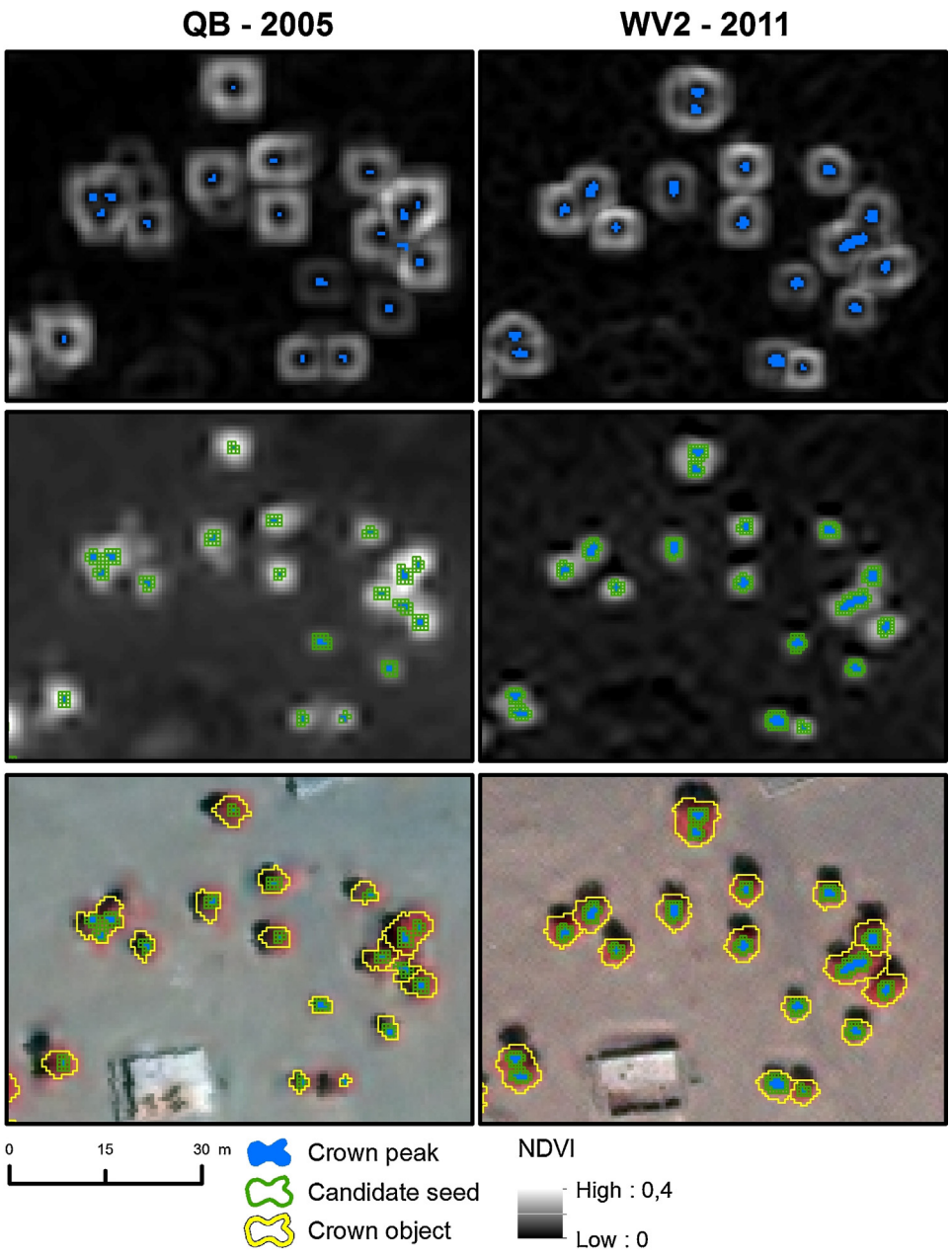

Fig. 3. Example of tree crowns delineated in the images of QB-2005 (left column) and WV2-2011 (right column). The top row images display the minimum/maximum filter band and the assigned crown peaks (step 2.4.2). The middle row images illustrates the NDVI band and derived candidate seeds (first iteration) (step 2.4.3) whereas the bottom row images show false colour composites with the final crown objects.

3.1. Descriptive analysis of field data

A total of 62 *P. euphratica* reference trees were measured in the field for change detection analysis. Descriptive statistics (Table 2) of the tree attributes indicate that on average tree heights increased from 6.9 to 7.6 m and the mean DBH rose from 29.5 to 34.2 cm. Crown diameters ranged from 2.5 to 7.2 m in 2005 and 2.4 to 7.7 m in 2011. The mean crown diameter increased from 4.4 m to 4.9 m over the last 6 years.

3.2. Tree crown detection

Table 3 shows the tree detection results obtained after applying a LM filter to both images. The large number of correctly

Table 2
Descriptive statistics for reference *P. euphratica* trees used in growth evaluation ($N = 62$).

	Height (m)				DBH (cm)				Tree crown diameter (m)			
	Min	Max	Mean	*SD*	Min	Max	Mean	*SD*	Min	Max	Mean	SD
2005	2.1	15.7	6.9	2.6	1.7	107.7	29.5	16.5	2.5	7.2	4.4	1.0
2011	3.2	13.6	7.6	2.3	6.0	111.0	34.2	17.9	2.4	7.7	4.9	1.3

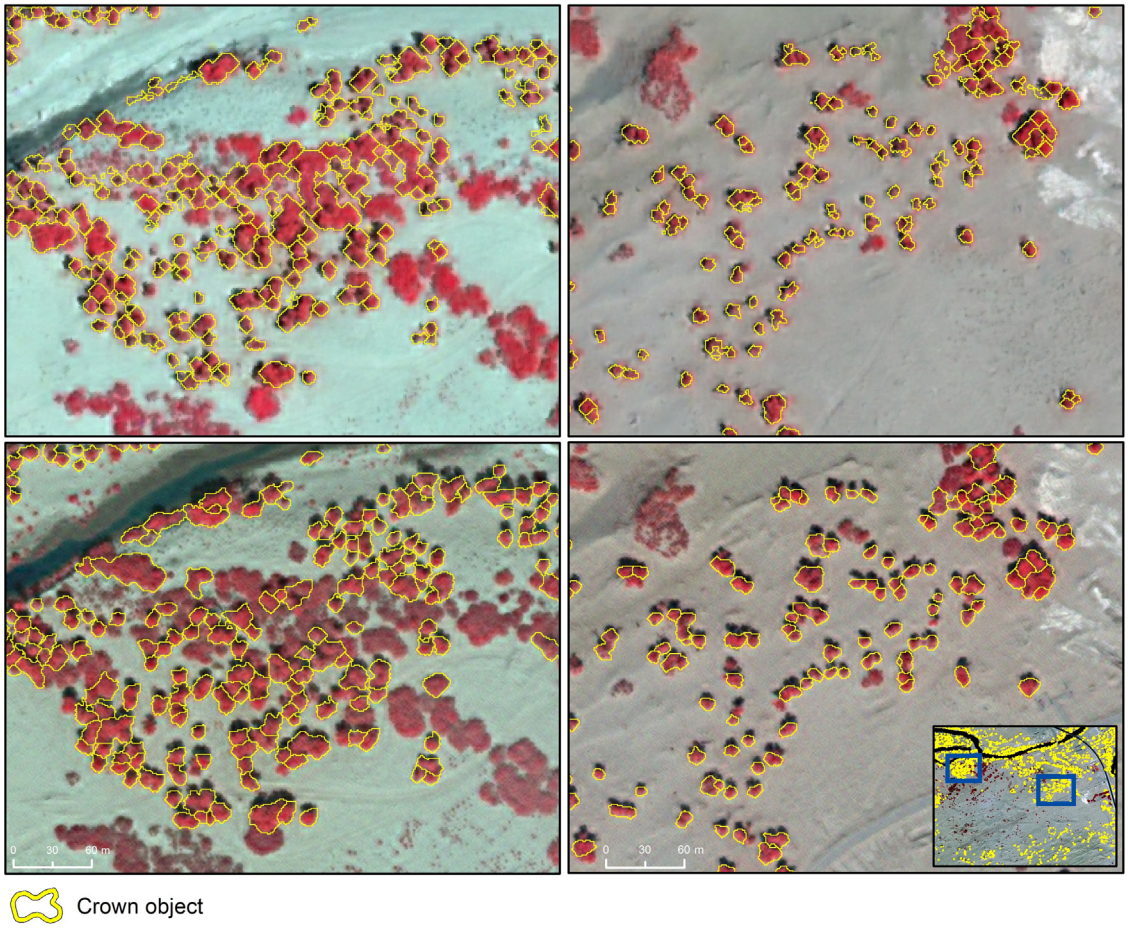

Fig. 4. Example of automatically delineated *P. euphratica* tree crowns in false colour composite QB (top row) and WV2 (bottom row) images. The overview map shows the location of the close up views within the study area.

identified tree crowns (QB: 54; WV2: 53) was achieved because of the absence of disturbing understorey vegetation, of similar spectral behaviour, and primarily isolated trees resulting in low forest complexity. However, by comparing the results of both images it can be concluded that in the QB image were more trees correctly identified than in the WV2 image. The error of omission (0:1) was low in both scenes and occurred only in areas with small tree crowns adjacent to medium trees. The maximum NDVI value of small trees is generally lower compared to medium size trees. If a small and medium sized tree occurs in one filter window instance, the small tree will be ignored and the medium sized tree gets the LM assigned. In neither of the two images was a false positive case identified. Errors of commission (2:1 or 3:1) occurred in 6 trees of the QB image and in 8 trees within the WV2 image.

3.3. Tree crown delineation

The conducted linear regression outlier test identified a total of three outliers (4.8% of the whole dataset) that appeared inconsistent with the remainder of the data. Because there was only one outlier in the 2005 data set and two outliers in the 2011 data set, the regression diagnostics identified these observations reliably (for all $p < 0.002$). All outlier were removed and 59 trees remained in the dataset. Data in Table 4 reveal that diameters from manually digitized crowns correspond better with field measurements than automatically extracted crowns. For both years the RMSE was lower ($RMSE_{2005}$: 0.96 m and $RMSE_{2011}$: 0.69 m) and R^2 higher (R^2_{2005}: 0.49 and R^2_{2011}: 0.75). This is, among other factors, because the diameter range of digitized crowns ($range_{2005}$: 1.62–6.15 cm; $range_{2011}$: 2.86–7.62 cm) is smaller than the diameter range of automatically extracted crowns ($range_{2005}$: 0.60–7.20 cm; $range_{2011}$: 2.38–7.62 cm). The magnitude of error for the automatically extracted crowns has approximately the size of two pan sharpened image pixels ($RMSE.QB_{2005}$: 1.16 m; $RMSE.WV2_{2011}$: 1.03 m).

Comparing diameters of individual crowns by means of their absolute difference, the difference between remote sensing derived (automatically extracted and manually digitized) and field measured crown diameters, indicated a greater crown diameter

Table 3
Results of tree detection using fixed size LM filter and mean difference to maximum NDVI > 0.03.

	Tree seed vs. reference crowns				
	0:1	1:0	1:1	2:1	3:1
QB – 2005	2	0	54	6	0
WV2 – 2011	1	0	53	5	3

Table 4
Mean crown diameter measurement error obtained from automated delineations and manually digitization compared with ground truth field data ($N = 59$, outliers removed).

	2005		2011	
Error measure	Automated	Digitized	Automated	Digitized
RMSE (m)	1.16	0.96	1.03	0.69
R^2	0.36	0.49	0.48	0.75

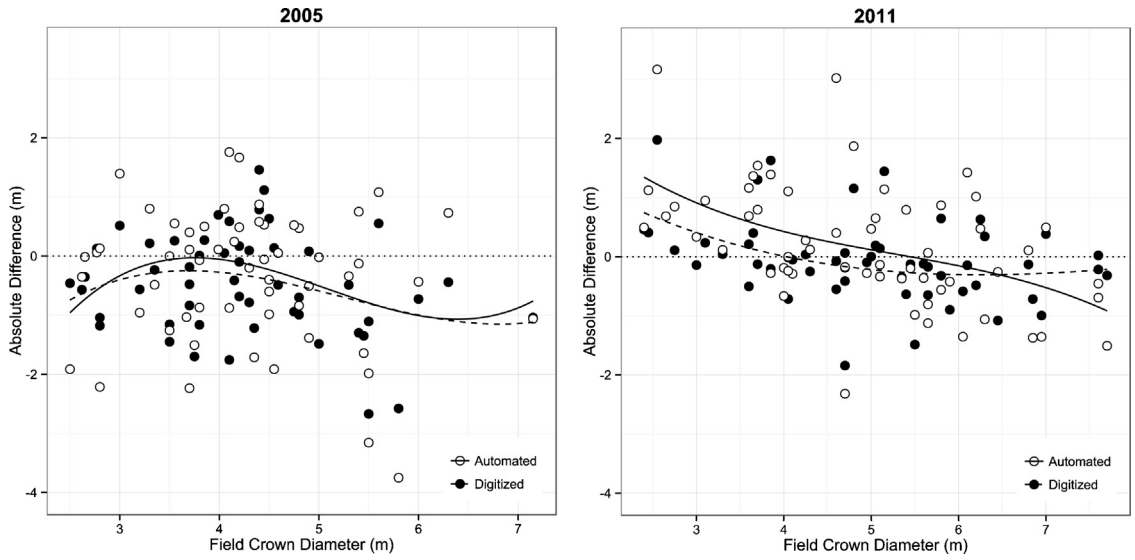

Fig. 5. The relation between absolute differences in crown diameter measured from automatically delineated and manually digitized crown diameters to ground-measured crown diameters (left: 2005; right: 2011). Third degree polynomial line graph summarizes the relationships; (digitized – solid black, automated – dashed black).

Table 5
Summary change statistics for *P. euphratica* crown diameters between 2005 and 2011 ($N = 59$).

Method	Crown diameter ($\bar{x}$)		Change crown diameter ($\bar{x}$)	95% Confidence interval for change ($\bar{x}$)	
	2005	2011	Total (annual)	Lower	Upper
Field (m)	4.29	4.90	0.61 (.10)	0.39	0.83 (±.22)
Digitized (m)	3.82	4.83	1.01 (.17)	0.78	1.24 (±.23)
Automated (m)	3.94	5.08	1.14 (.19)	0.81	1.47 (±.33)

underestimation in 2005 and an evenly balanced crown diameter estimation in 2011 (Fig. 5). Equally for both years, larger crowns tended to be more underestimated by the automated delineation approach. For 2011 there was a minor overestimation of small crowns. In 2005, small crowns were slightly underestimated. However, the automated delineation results were not significantly different from those manually digitized (p.2005: 0.49; p.2011: 0.11).

3.4. Change detection

Table 5 summarizes the detected changes of *P. euphratica* crown diameters between 2005 and 2011. An overall crown diameter rise was detected in all methods. The field measured results indicated a crown diameter growth of 0.61 m on average. Considering the field measured data as reference, the automatic delineation method overestimated crown diameters by 0.53 m while the diameters of manually digitized crowns were overestimated by 0.4 m, on average. The main reason for overrating is the crown diameter underestimation in 2005 from the QB scene. The automated region growing approach underestimated crowns by 0.35 m and the digitizing method underestimated crowns by 0.47 m, on average (Fig. 6). On a single tree level were negative crown diameter changes of up to 2.3 m and positive crown diameter changes of up to 4 m observed.

A scatter diagram and a crown diameter change distribution were used to determine the relationship between crown diameter measurements from 2005 and 2011 (Fig. 7). All points left from the 1:1 black reference line indicate a crown diameter increase; points on the other side indicate a decrease. The results in Fig. 7 indicate that projected points cluster closely around their mean for field collected crown diameter (SD_{change}: 0.85) and manually digitized crown diameter (SD_{change}: 0.89) while projected points of the automatic delineation (SD_{change}: 1.28) are further away from their mean. Points beyond the 95% confidence interval may be subject to errors, and those errors contribute to the uncertainty of the measurements.

4. Discussion

In this study, we applied an object based change detection method to a semiarid open *P. euphratica* Tugai forest, aiming to quantify the rate of tree crown changes over a period of six years. The implemented OBIA approach produced meaningful image objects that resemble *P. euphratica* tree crowns (Fig. 4). Our results demonstrate that derived tree crown diameter estimates from VHSR imagery agree reasonably well with field reference data, with an average RMSE of 1.16 m (2005) and 1.03 m (2011) and can therefore support field based tree crown monitoring efforts. Essential characteristics of the applied method and the obtained results are discussed below.

4.1. Field reference data

Various factors may influence the accuracy of tree diameter estimation in this study. One of the most probable source of error are the in-situ measured reference data for accuracy validation. These data are not 'ground truth', as it is often erroneously referred to (Foody, 2010), but may contain uncertainty (Richter et al., 2011). Our field data were collected in 2005 and 2011 by two different groups of people, using the same measurement process. Assuming both groups measured carefully and precisely, differing

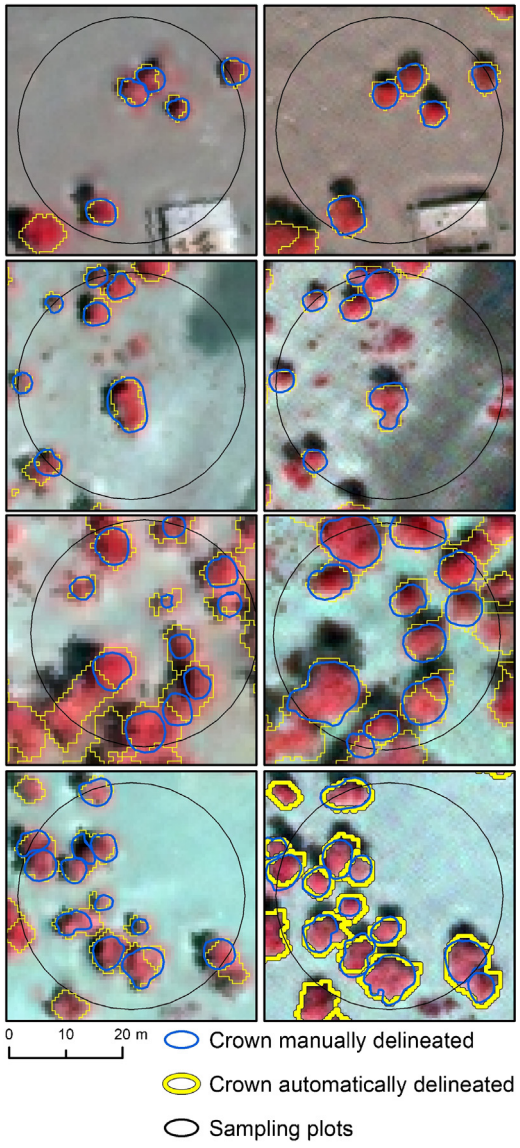

Fig. 6. Example of 4 study plots (black) with automatically (yellow) and manually (blue) delineated *P. euphratica* tree crowns in false colour composite QB (left column) and WV2 (right column) images. (For interpretation of the references to colour in the text, the reader is referred to the web version of this article.)

interpretation of the same object may result in subjectivity and bias. How accurate can a vague or rather fuzzy crown border be measured when difficulties arise in defining the 'exact' crown boundary in the field? Lam et al. (2011) observed for the studied *P. euphratica* stand, that the general crown shape varies from relatively dense hemispherical shapes for young and healthy trees to wide open jagged, serrated shapes for older trees. Several old trees lost the top portion of the crown, and some of them formed patches of secondary crowns from dormant buds. When seen from space, these disperse crown forms are not observed as round and may be underrepresented by only two crown diameter measurements. We therefore propose to increase the field crown diameter measurements to four diameter measurements, 45° apart from each other as it is carried out during stand area determinations (Röhle, 1986).

4.2. Tree crown detection and delineation

The heterogeneous crown form of *P. euphratica* was frequently accompanied by a high within-crown spectral variability. The canopy reflectance plunged in parts of dead primary crowns, lacking photosynthetic material while reflectance rose in parts with foliated secondary crowns. This caused crowns to differ from the typical ellipsoidal crown shapes of other deciduous tree species. The spectral responses to the irregular branch pattern were multiple reflectance peaks, especially in sub-meter resolution imagery (Pouliot et al., 2002). In fact, in 10% of the analyzed trees (QB scene, 2005) we obtained at least two reflectance peaks per tree (13% in WV2 scene, 2011). The rising number of multiple reflectance peaks was expected due to the increase of within crown variability with higher spatial and spectral resolution (from 0.6 m to 0.5 m). To illustrate the issue, Fig. 8 presents a three-dimensional view of NDVI values for two trees, one with an irregular crown structure (right) and one medium sized tree with a homogeneous tree crown (left). In normal procedure a tree with three reflectance peaks (crown peaks highlighted in red, Fig. 8) would have caused an error of commission (3:1 error). In our case the detection of multiple reflectance peaks in an irregular shaped crown should not be considered as commission error because those peaks exist. However, difficulties arise when to validate detected reflectance peaks in the field. Extracting individual vertical structure of tree crowns from LiDAR would improve the analysis since reliable tree height and treetop data are detectable (Chen et al., 2006b). We did not find literature information concerning the distance between LiDAR measured treetop data and crown peaks from sunlit reflectance maxima.

The high accuracy of the individual tree detection that we obtained are consistent with those of Whiteside and Ahmad (2008), who achieved a local maxima seed detection in Eucalypt dominant savannah with a user accuracy of 84.3% and a producers accuracy of 96.3% within a QB image. In Zhou et al. (2012) field validated detection rate exceeded 82% in Eucalyptus plantation with WV2. In our study, 1:1 detection success ranged from 85.5% in WV2 to 87.1% in QB. The essential difference between above mentioned surveys was because of the existence of undergrowth, shrubs and annual grasses and the homogeneous tree spacing due to plantation outlines.

The crown diameter from the manually digitized tree crowns agreed better with the field reference data than the results from automated delineation approach. However, the OBIA approach achieved RMSE in both sensor types below two image pixels (Table 4). These accuracy levels are similar with studies which compared their results to field-measured crown areas rather than manually digitized reference trees (Pouliot et al., 2002, 2005; Song et al., 2010). One source of error is related to the mixed pixel effect which occurs in the vicinity of the crown boundary and influences the crown boundary delineation result. Mixed pixels tend to smooth reflectance variability and cause tree crown overestimation if included and underestimation if excluded (Rocchini et al., 2013). In our results, the measurements of the crown diameter touch the crown boundary in two sides of the crown axis, therefore appears the mixed pixel effect twice. For the bi-temporal tree crown change detection we selected two peak green summer images because of their adequate quality as well as the phenological stability (Coppin et al., 2004). The quality of the QB image was slightly reduced after the HCS image fusion process due to small NIR artefacts, observed close to tree crown edges.

We also found that the region growing algorithm works better at isolated or scattered trees than in dense or closed forest areas. A uncertainty factor for the crown delineation method is the fact that the method dependence on the presence of crowns peaks. A tree crown peak is almost certainly found at isolated trees, but in dense or closed stocks are situations were a dominant tree covers its neighbour and its peak will remains undetected. The consequence is that the region growing method segments over the dominated tree and the resulting tree crown appears rather big and unshapely.

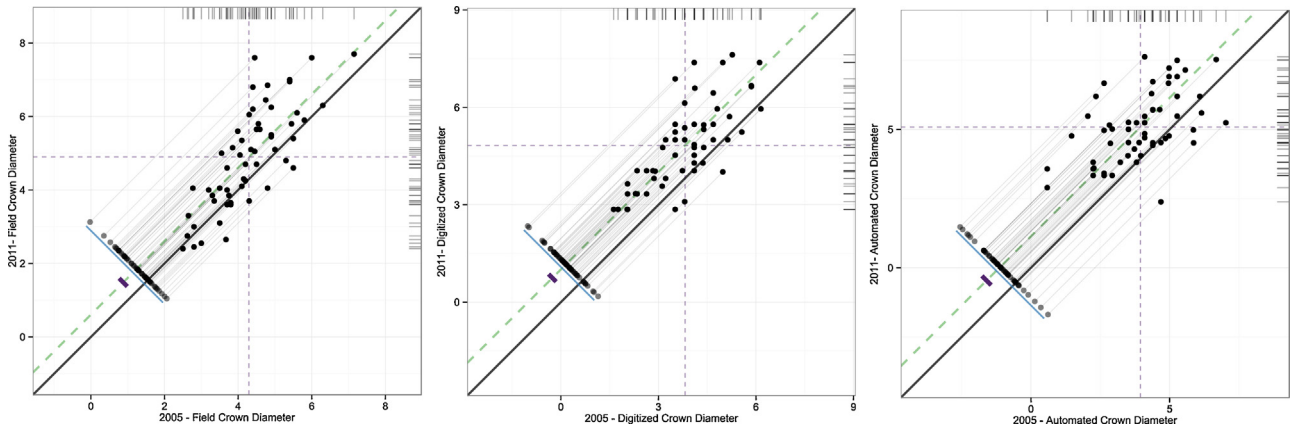

Fig. 7. Scatterplots of crown diameters in 2005 (*x* axis) and 2011 (*y* axis) illustrate the change detected for each method. A 1:1 reference line is drawn as black solid line. Semi-transparent 'shadow' points show the distribution of change scores with thin grey lines leading from each raw measurement point to its shadow projection on the change distribution. The range of the change distribution is drawn as a blue line beneath the shadow points. Averages for 2005 and 2011 crown diameters are plotted as thin dashed vertical and horizontal lines. Rug plots are presented for the distributions of 2005 (at the top of graphic) and 2011 (on the right side). The 95% confidence interval for the change results is shown as a green dashed band. Field measured (left); manually digitized (middle); automatically delineated (right). (For interpretation of the references to colour in the text, the reader is referred to the web version of this article.)

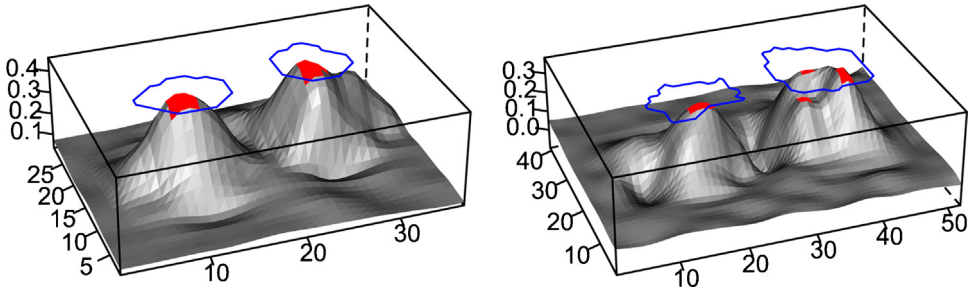

Fig. 8. Tree crown detection results for two trees. Tree peaks (red), manually delineated crown (blue) (QB – 2005 (left), WV2 – 2011 (right); Axis labels: *x* and *y* – in pixel, *z*: NDVI values). (For interpretation of the references to colour in the text, the reader is referred to the web version of this article.)

4.3. Change of vegetation cover

The long term ecological restoration of degraded riparian Tugai forests along the lower reaches of the Tarim river has beneficial influence on the *P. euphratica* population. Our findings confirmed a positive tree crown growth and suggest a crown diameter increase of 1.14 m, on average. The detected expansion of above ground green biomass corresponds to natural succession and suggests improved groundwater conditions after Ecological Water Diversion from 2000 until 2011 (Zhandong et al., 2009). The results of the automatic tree crown delineation show a moderate relation to the reference data (with (R^2_{2005}: 0.36 and (R^2_{2011}: 0.48) but can be considered useful due to a similar magnitude of the error like the manually digitized results. The OBIA method proved to be applicable in arid environments with scattered trees such as the sparse riparian Tugai forests and showed great suitability to evaluate ecological restoration efforts in a remote ecosystem.

5. Conclusion and outlook

We used two very high resolution satellite images to quantify recent tree crown diameter changes in a degraded riparian Tugai forest in north-western China. Our results suggest a positive tree crown growth with an average crown diameter increase of 1.14 m. On a single tree basis, small crowns were slightly underestimated in QB and overestimated in WV2. Tree crown diameters of larger crowns were generally underestimated. The results of the automated tree crown delineation show a moderate relation to 59 reference trees measured in the field (R^2_{2005}: 0.36 and R^2_{2011}: 0.48). The automated OBIA method proved to be applicable in scenes of both evaluated sensors for sparse riparian Tugai forest, especially in feature extraction of individual tree crowns and produced useful results.

Acknowledgements

This work was funded by The Federal Ministry of Education and Research Fund (Grant number: 01LL0918G). We are very grateful to Mai Ruhl, Niu Ting, Duan and Abdimijit Ablekim for the help and the involvement in the fieldwork.

References

Ardila, J.P., Bijker, W., Tolpekin, V.A., Stein, A., 2012a. Context-sensitive extraction of tree crown objects in urban areas using VHR satellite images. Int. J. Appl. Earth Observ. Geoinform. 15, 57–69, http://dx.doi.org/10.1016/j.jag.2011.06.005.

Ardila, J.P., Bijker, W., Tolpekin, V.A., Stein, A., Nov 2012b. Quantification of crown changes and change uncertainty of trees in an urban environment. ISPRS J. Photogram. Remote Sens. 74, 41–55, http://dx.doi.org/10.1016/j.isprsjprs.2012.08.007.

Blaschke, T., 2010. Object based image analysis for remote sensing. ISPRS J. Photogram. Remote Sens. 65, 2–16, http://dx.doi.org/10.1016/j.isprsjprs.2009.06.004.

Blaschke, T., Johansen, K., Tiede, D., 2011. Object-based image analysis for vegetation mapping and monitoring. In: Weng, Q. (Ed.), Advances in Environmental Remote Sensing: Sensors, Algorithms, and Applications. CRC Press Taylor & Francis Group, Boca Raton, FL, United States, pp. 241–271.

Breiman, L., Friedman, J., Stone, C.J., Olshen, R.A., 1984. Classification and Regression Trees. CRC Press LLC, Boca Raton, Florida, United States, No. ISBN 0412048418.

Bright, B.C., Hicke, J.A., Hudak, A.T., 2012. Estimating aboveground carbon stocks of a forest affected by mountain pine beetle in Idaho using lidar and multispectral imagery. Remote Sens. Environ. 124, 270–281, http://dx.doi.org/10.1016/j.rse.2012.05.016.

Bunting, P., Lucas, R., 2006. The delineation of tree crowns in Australian mixed species forests using hyperspectral Compact Airborne Spectrographic Imager (CASI) data. Remote Sens. Environ. 101, 230–248, http://dx.doi.org/10.1016/j.rse.2005.12.015.

Chen, Q., Baldocchi, D., Gong, P., Kelly, M., 2006a. Isolating individual trees in a savanna woodland using small footprint lidar data. Photogram. Eng. Remote Sens. 72, 923–932.

Chen, Y.-N., Zilliacus, H., Li, W.-H., Zhang, H.-F., Chen, Y.-P., 2006b. Groundwater level affects plant species diversity along the lower reaches of the Tarim River, Western China. J. Arid Environ. 66, 231–246, http://dx.doi.org/10.1016/j.jaridenv.2005.11.009.

Chubey, M.S., Franklin, S.E., Wulder, M.A., 2006. Object-based analysis of ikonos-2 imagery for extraction of forest inventory parameters. Photogram. Eng. Remote Sens. 72, 383.

van Coillie, F.M.B., Devriendt, F., De Wulf, R.R., 2012. Directional local filtering assisting individual tree analysis in closed forest canopies using VHR optical and LiDAR data. In: Proceedings of the 4th GEOBIA, Rio de Janeiro - Brazil, pp. 350–354.

Coppin, P., Jonckheere, I., Nackaerts, K., Muys, B., Lambin, E., 2004. Review article: digital change detection methods in ecosystem monitoring: a review. Int. J. Remote Sens. 25, 1565–1596, http://dx.doi.org/10.1080/0143116031000101675.

Culvenor, D.S., 2002. TIDA: an algorithm for the delineation of tree crowns in high spatial resolution remotely sensed imagery. Comp. Geosci. 28, 33–44, URL http://www.sciencedirect.com/science/article/pii/S0098300400001102

Desclée, B., Bogaert, P., Defourny, P., 2006. Forest change detection by statistical object-based method. Remote Sens. Environ. 102, 1–11, http://dx.doi.org/10.1016/j.rse.2006.01.013.

Cognition, 2010. Ruleset: Conditional Quad Tree Segmentation. http://community.ecognition.com/home/conditional_quad_tree_v102_141.dcp

eCognition, 2012a. Trimble. "eCognition Developer 8.8. 1: Reference Book." Trimble Germany GmbH, Munich, Germany.

eCognition, 2012b. Trimble. "eCognition Developer 8.8. 1 User Guide." Trimble Germany GmbH, Munich, Germany.

Falkowski, M.J., Wulder, M.A., White, J.C., Gillis, M.D., 2009. Supporting large-area, sample-based forest inventories with very high spatial resolution satellite imagery. Prog. Phys. Geogr. 33, 403–423, http://dx.doi.org/10.1177/0309133309342643.

Foody, G.M., 2010. Assessing the accuracy of land cover change with imperfect ground reference data. Remote Sens. Environ. 114, 2271–2285, http://dx.doi.org/10.1016/j.rse.2010.05.003.

Gebreslasie, M., Ahmed, F., Van Aardt, J.A., Blakeway, F., 2011. Individual tree detection based on variable and fixed window size local maxima filtering applied to IKONOS imagery for even-aged Eucalyptus plantation forests. Int. J. Remote Sens. 32, 4141–4154, http://dx.doi.org/10.1080/01431161003777205.

Gitelson, A., Merzlyak, M.N., 1994. Spectral reflectance changes associated with autumn senescence of *Aesculus hippocastanum L.* and *Acer platanoides L.* leaves. Spectral features and relation to chlorophyll estimation. J. Plant Physiol. 143, 286–292, http://dx.doi.org/10.1016/S0176-1617(11)81633-0.

Gitelson, A.A., Kaufman, Y.J., Merzlyak, M.N., 1996. Use of a green channel in remote sensing of global vegetation from EOS-MODIS. Remote Sens. Environ. 58, 289–298, http://dx.doi.org/10.1016/S0034-4257(96)00072-7.

Gougeon, F.A., Leckie, D.G., 2006. The individual tree crown approach applied to Ikonos images of a coniferous plantation area. Photogram. Eng. Remote Sens. 72, 1287–1297.

Gougeon, F.A., Moore, T.,1988. Individual tree classification using Meis-II imagery. In: Geoscience and Remote Sensing Symposium. IGARSS'88. Remote Sensing: Moving Toward the 21st Century., International. IEEE, http://dx.doi.org/10.1109/IGARSS.1988.570478.

Hirata, Y., 2008. Estimation of stand attributes in *Cryptomeria japonica* and *Chamaecyparis obtusa* stands using QuickBird panchromatic data. J. Forest Res. 13, 147–154, http://dx.doi.org/10.1007/s10310-008-0059-7.

Huete, A., 1988. A soil-adjusted vegetation index (SAVI). Remote Sens. Environ. 25, 295–309, http://dx.doi.org/10.1016/0034-4257(88)90106-X.

Jordan, C.F., 1969. Derivation of leaf-area index from quality of light on the forest floor. Ecology, 663–666.

Katoh, M., Gougeon, F.A., 2012. Improving the precision of tree counting by combining tree detection with crown delineation and classification on homogeneity guided smoothed high resolution (50 cm) multispectral airborne digital data. Remote Sens. 4, 1411–1424, http://dx.doi.org/10.3390/rs4051411.

Ke, Y., Quackenbush, L.J., 2011a. A comparison of three methods for automatic tree crown detection and delineation from high spatial resolution imagery. Int. J. Remote Sens. 32, 3625–3647, http://dx.doi.org/10.1080/01431161003762355.

Ke, Y., Quackenbush, L.J., 2011b. A review of methods for automatic individual tree-crown detection and delineation from passive remote sensing. Int. J. Remote Sens. 32, 4725–4747, http://dx.doi.org/10.1080/01431161.2010.494184.

Kennedy, R.E., Cohen, W.B., Schroeder, T.A., 2007. Trajectory-based change detection for automated characterization of forest disturbance dynamics. Remote Sens. Environ. 110, 370–386, http://dx.doi.org/10.1016/j.rse.2007.03.010.

Krause, K., 2005. Radiometric Use of QuickBird Imagery. Technical note. DigitalGlobe, 1601 Dry Creek Drive Suite 260, Longmont, Colorado 80503, USA.

Laliberte, A.S., Fredrickson, E.L., Rango, A., 2007. Combining decision trees with hierarchical object-oriented image analysis for mapping arid rangelands. Photogram. Eng. Remote Sens. 73, 197.

Lam, T.Y., Kleinn, C., Coenradie, B., 2011. Double sampling for stratification for the monitoring of sparse tree populations: the example of *P. euphratica* Oliv. forests at the lower reaches of Tarim River, Southern Xinjiang, China. Environ. Monitor. Assess. 175, 45–61, http://dx.doi.org/10.1007/s10661-010-1492-6.

Leckie, D.G., Gougeon, F.A., Hill, D., Quinn, R., Armstrong, L., Shreenan, R., 2003. Combined high-density lidar and multispectral imagery for individual tree crown analysis. Can. J. Remote Sens. 29, 633–649, http://pubs.casi.ca/doi/abs/10.5589/m03-024.

Leckie, D.G., Gougeon, F.A., Tinis, S., Nelson, T., Burnett, C.N., Paradine, D., 2005. Automated tree recognition in old growth conifer stands with high resolution digital imagery. Remote Sens. Environ. 94, 311–326, http://dx.doi.org/10.1016/j.rse.2004.10.011.

Leckie, D.G., Gougeon, F.A., Walsworth, N., Paradine, D., 2003b. Stand delineation and composition estimation using semi-automated individual tree crown analysis. Remote Sens. Environ. 85, 355–369, http://dx.doi.org/10.1016/S0034-4257(03)00013-0.

Leckie, D.G., Jay, C., Gougeon, F.A., Sturrock, R., Paradine, D., 2004. Detection and assessment of trees with *Phellinus weirii* (laminated root rot) using high resolution multi-spectral imagery. Int. J. Remote Sens. 25, 793–818, http://dx.doi.org/10.1080/0143116031000139926.

McFeeters, S., 1996. The use of the Normalized Difference Water Index (NDWI) in the delineation of open water features. Int. J. Remote Sens. 17, 1425–1432, http://dx.doi.org/10.1080/01431169608948714.

Mora, B., Wulder, M.A., White, J.C., Hobart, G., 2013. Modeling stand height, volume, and biomass from very high spatial resolution satellite imagery and samples of airborne LiDAR. Remote Sens. 5, 2308–2326, http://dx.doi.org/10.3390/rs5052308.

Niccolai, A., Hohl, A., Niccolai, M., Oliver, C.D., 2010. Integration of varying spatial, spectral and temporal high-resolution optical images for individual tree crown isolation. Int. J. Remote Sens. 31, 5061–5088, http://dx.doi.org/10.1080/01431160903283850.

Olsson, H., Egberth, M., Engberg, J., Fransson, J.E., Pahlén, T.G., Hagner, O., Holmgren, J., Joyce, S., Magnusson, M., Nilsson, B., et al., 2005. Current and emerging operational uses of remote sensing in swedish forestry. In: Proceedings of the Seventh Annual Forest Inventory and Analysis Symposium, USDA Forest Serv. Gen. Tech. Rep. WO-69, pp. 39–46.

Ozdemir, I., 2008. Estimating stem volume by tree crown area and tree shadow area extracted from pan-sharpened Quickbird imagery in open Crimean juniper forests. Int. J. Remote Sens. 29, 5643–5655, http://dx.doi.org/10.1080/01431160802082155.

Padwick, C., Deskevich, M., Pacifici, F., Smallwood, S., April 2010. WorldView-2 Pan-Sharpening. In: American Society for Photogrammetry and Remote Sensing, San Diego, California.

Pouliot, D.A., King, D.J., Bell, F.W., Pitt, D.G., 2002. Automated tree crown detection and delineation in high-resolution digital camera imagery of coniferous forest regeneration. Remote Sens. Environ. 82, 322–334, http://dx.doi.org/10.1016/S0034-4257(02)00050-0.

Pouliot, D.A., King, D.J., Pitt, D.G., 2005. Development and evaluation of an automated tree detection delineation algorithm for monitoring regenerating coniferous forests. Can. J. Forest Res. 35, 2332–2345, http://dx.doi.org/10.1139/X05-145.

Qi, J., Chehbouni, A., Huete, A., Kerr, Y., Sorooshian, S., 1994. A modified soil adjusted vegetation index. Remote Sens. Environ. 48, 119–126, http://dx.doi.org/10.1016/0034-4257(94)90134-1.

Richter, K., Hank, T.B., Atzberger, C., Mauser, W., 2011. Goodness-of-fit measures: what do they tell about vegetation variable retrieval performance from Earth observation data. In: Proc. SPIE, http://dx.doi.org/10.1117/12.897980.

Rocchini, D., Foody, G.M., Nagendra, H., Ricotta, C., Anand, M., He, K.S., Amici, V., Kleinschmit, B., Förster, M., Schmidtlein, S., et al., 2013. Uncertainty in ecosystem mapping by remote sensing. Comp. Geosci. 50, 128–135, http://dx.doi.org/10.1016/j.cageo.2012.05.022.

Röhle, H., 1986. Vergleichende Untersuchungen zur Ermittlung der Genauigkeit bei der Ablotung von Kronenradien. Forstarchiv 57, 67–71.

Rondeaux, G., Steven, M., Baret, F., 1996. Optimization of soil-adjusted vegetation indices. Remote Sens. Environ. 55, 95–107.

Sader, S.A., Bertrand, M., Wilson, E.H., 2003. Satellite change detection of forest harvest patterns on an industrial forest landscape. Forest Sci. 49, 341–353, URL http://www.ingentaconnect.com/content/saf/fs/2003/00000049/00000003/art00002

van der Sande, C.J., 2010. Automatic object recognition and change detection of urban trees. Int. Arch. Photogram. Remote Sens. Spatial Inform. Sci. XXXVIII-4/C7.

Sims, D.A., Gamon, J.A., 2002. Relationships between leaf pigment content and spectral reflectance across a wide range of species, leaf structures and developmental stages. Remote Sens. Environ. 81, 337–354, http://dx.doi.org/10.1016/S0034-4257(02)00010-X.

Song, C., Dickinson, M.B., Su, L., Zhang, S., Yaussey, D., 2010. Estimating average tree crown size using spatial information from Ikonos and QuickBird images: across-sensor and across-site comparisons. Remote Sens. Environ. 114, 1099–1107, http://dx.doi.org/10.1016/j.rse.2009.12.022.

Thevs, N., Buras, A., Zerbe, S., Kühnel, E., Abdusalih, N., Ovezberdiyeva, A., 2012. Structure and wood biomass of near-natural floodplain forests along the Central Asian rivers Tarim and Amu Darya. Forestry 85, 193–202, http://dx.doi.org/10.1093/forestry/cpr056.

Tiede, D., Lang, S., Hoffmann, C., 2008. Type-specific class modelling for one-level representation of single trees. In: Blaschke, T., Lang, S., Hay, G. (Eds.), Object-Based Image Analysis – Spatial Concepts for Knowledge-Driven Remote Sensing Applications. Springer, Berlin, pp. 133–151.

Tucker, C.J., 1979. Red and photographic infrared linear combinations for monitoring vegetation. Remote Sens. Environ. 8, 127–150, http://dx.doi.org/10.1016/0034-4257(79)90013-0.

Updike, T., Comp, C., 2010. Radiometric Use of WorldView-2 Imagery, Technical Note 1.0, DigitalGlobe.

Wang, L., Gong, P., Biging, G.S., 2004. Individual tree-crown delineation and treetop detection in high-spatial-resolution aerial imagery. Photogram. Eng. Remote Sens. 70, 351–358.

Weisgerber, H., 1994. *Populus euphratica*. Enzyklopädie der Holzgewächse: Handbuch und Atlas der Dendrologie. Ecomed, Landsberg am Lech 22, 39–41.

Whiteside, T., Ahmad, W., 2008. Estimating canopy cover from eucalypt dominant tropical savanna using the extraction of tree crowns from very high resolution imagery. In: Proceedings of GEOBIA 2008 – Pixels, Objects, Intelligence: GEOgraphic Object-Based Image Analysis for the 21st Century, Calgary.

Wulder, M., Niemann, K.O., Goodenough, D.G., 2000. Local maximum filtering for the extraction of tree locations and basal area from high spatial resolution imagery. Remote Sens. Environ. 73, 103–114, http://dx.doi.org/10.1016/S0034-4257(00)00101-2.

Wulder, M.A., White, J.C., Niemann, K.O., Nelson, T., 2004. Comparison of airborne and satellite high spatial resolution data for the identification of individual trees with local maxima filtering. Int. J. Remote Sens. 25, 2225–2232, http://dx.doi.org/10.1080/01431160310001659252.

Zhandong, S., Opp, C., Run, W., 2009. Vegetation response to Ecological Water Diversion in the lower Tarim River, Xinjiang, China. Basic Appl. Dryland Res. 3, 1–16, ISSN 1864-3191.

Zhou, J., Proisy, C., Descombes, X., Le Maire, G., Nouvellon, Y., Stape, J.-L., Viennois, G., Zerubia, J., Couteron, P., 2012. Mapping local density of young *Eucalyptus* plantations by individual tree detection in high spatial resolution satellite images. Forest Ecol. Manage., http://dx.doi.org/10.1016/j.foreco.2012.10.007.

Zhou, W., Yang, X., Hao, P., Liu, Q., Cao, D., Baribault, T., Li, J., 2010. Plant diversity and its maintenance in *Populus euphratica* riparian forests in the Ejina Oasis, China. Forestry Studies China 12, 55–61, http://dx.doi.org/10.1007/s11632-010-0011-8.